

doi: 10.12029/gc20160404

国显正, 贾群子, 李金超, 等. 东昆仑热水钼矿区似斑状黑云母二长花岗岩元素地球化学及年代学研究[J]. 中国地质, 2016, 43(4): 1165-1177.
Guo xianzheng, Jia qunzi, Li jincao, et al. Geochemical characteristics and geochronology of porphyroid biotite monzogranite from the Reshui Mo polymetallic deposit, East Kunlun Mountains[J]. Geology in China, 2016, 43(4): 1165-1177 (in Chinese with English abstract).

东昆仑热水钼矿区似斑状黑云母二长花岗岩元素地球化学及年代学研究

国显正^{1,2} 贾群子² 李金超² 孔会磊² 栗亚芝² 许荣科¹ 南卡俄吾³

(1. 中国地质大学(武汉)地质调查研究院, 湖北 武汉 430074; 2. 中国地质调查局西安地质调查中心, 陕西 西安 710054;
3. 陕西省土地工程建设集团有限责任公司, 陕西 西安 710075)

摘要:热水钼矿区处于东昆仑造山带东段, 大地构造位置位于北昆仑岩浆弧, 区内侵入岩较发育, 其中与热水钼多金属矿密切相关的矿化似斑状黑云母二长花岗岩岩相学及地球化学数据显示, SiO_2 含量在 67.64%~71.09%, 铝饱和指数(A/CNK)为 0.86~1.11, 为准铝质到过铝质, $\text{K}_2\text{O}/\text{Na}_2\text{O}$ 值 1.35~2.32, 里特曼指数为 1.73~1.99, 属于高钾钙碱性 I 型花岗岩。岩石总体上富集大离子亲石元素 Rb、Th、U、K、Pb 等, 明显亏损高场强元素 Ta、Nb、Ce 等, 贫 P、Ti。稀土元素总量(ΣREE)为 94.27×10^{-6} ~ 127.44×10^{-6} , 平均为 110.92×10^{-6} , 稀土元素配分曲线呈右倾型, 具有较明显的轻稀土富集、重稀土亏损的特征, 弱到中等程度的负铈异常。LA-ICP-MS 锆石 U-Pb 年龄为 (230.9 ± 1.4) Ma, 形成于印支期, 钼多金属矿与这一时期岩浆活动密切相关。综合分析表明, 似斑状黑云母二长花岗岩形成构造体制转换阶段, 在热水地区具有寻找斑岩型矿床潜力。

关键词:似斑状黑云母二长花岗岩; 地球化学; 锆石 U-Pb 定年; 热水钼矿区

中图分类号: P588.12¹; P597 文献标志码: A 文章编号: 1000-3657(2016)04-1165-13

Geochemical characteristics and geochronology of porphyroid biotite monzogranite from the Reshui Mo polymetallic deposit, East Kunlun Mountains

GUO Xian-zheng^{1,2}, JIA Qun-zi², LI Jin-chao², KONG Hui-lei², LI Ya-zhi², XU Rong-ke¹,
Namhka Norbu³

(1. Institute of Geological Survey, China University of Geosciences, Wuhan, 430074, Hubei, China; 2. Xi'an Center of Geological Survey, CGS, Xi'an 710054, Shaanxi, China; 3. Shaanxi Land Engineering Construction Group, Xi'an 710075, Shaanxi, China)

Abstract: The Reshui Mo polymetallic deposit is located at the North Kunlun magmatic arc, where lots of intrusive rocks occur. Geochemical data reveal that the porphyroid biotite monzogranite from East Kunlun is rich in silicon (67.64%–71.09%), Al_2O_3 ,

收稿日期: 2015-10-08; 改回日期: 2016-03-07

基金项目: 中国地质调查局地质调查项目(12120113029000, 12120115021501, DD20160013)资助。

作者简介: 国显正, 男, 1990 年生, 硕士生, 矿产普查与勘探专业, 从事成矿规律研究; E-mail: cuggxz@126.com。

通讯作者: 贾群子, 男, 1962 年生, 研究员, 从事矿床学和区域成矿规律研究; E-mail: xajqunzi@126.com。

(13.8%–14.57%), Na_2O (2.23%–3.02%), and K_2O (3.95%–5.18%), with ratios of $\text{K}_2\text{O}/\text{Na}_2\text{O}$ being 1.35–2.32 and A/CNK being 0.86–1.11, 1.01 on average, suggesting that the granite should belong to high potassic calc-alkaline and I type granite. The porphyroid biotite monzogranite is intensively depleted in HFSE (Ta, Nb, mCe), enriched in LILE (Rb, Th, U, K, Pb), and poor in P, Ti. The total rare earth elements (ΣREE) are 94.27×10^{-6} – 127.44×10^{-6} , with an average of 110.92×10^{-6} . The rare earth element distribution curve shows the right-inclined type, and has characteristics of obvious enrichment of light rare earth and depletion of heavy rare earth elements. LA-ICP-MS zircon U–Pb dating shows that the formation age of the rock is (230.9 ± 1.4) Ma, belonging to Indosinian stage. The molybdenum polymetallic deposit is closely related to the magmatic activity during this period. Based on tectonic history and the structure environment in combination with the geochemical characteristics, the authors hold that the porphyritic biotite monzonitic granite of the Reshui deposit was formed at the structural transformation stage, and Reshui area has potential for finding porphyry deposits.

Key words: porphyroid biotite monzogranite; geochemistry; zircon U–Pb dating; Reshui molybdenum polymetallic deposit

About the first author: GUO Xian-zheng, male, born in 1990, master, engages in the study of metallogenic regularity; E-mail: cuggxz@163.com.

About the corresponding author: JIA Qun-zi, male, born in 1962, professor, engages in the study of ore deposits and metallogenic regularity; E-mail: xajqunzi@126.com.

Fund Support: Supported by China Geological Survey programs (No. 12120113029000, No. 12120115021501, DD20160013).

东昆仑造山带位于青藏高原北部,区内构造形迹以断裂为主,自南向北主要有3条区域性断裂,昆南-昆北-昆中断裂带;该造山带内岩浆岩广泛出露,岩浆活动可划分出4期:晋宁期、加里东期、晚华力西-印支期和燕山期^[1-3],前人已进行了相关研究^[4-15];岩浆活动与成矿密切相关,已有众多学者论述^[16-32],其中印支期是该地区最为重要的构造-岩浆-成矿作用活跃期^[5]。

热水钼多金属矿是近几年来勘查评价的一个矿床,热水地区的哈日扎铜铅锌矿花岗闪长斑岩形成年龄 (234.5 ± 4.8) Ma^[33],哈陇休玛钨钼矿花岗闪长斑岩形成时代 (230 ± 1) Ma^[34],而热水钼矿区似斑状黑云母二长花岗岩形成时代尚不清楚,前人根据区域地质资料认为其形成于华力西期,但其侵位时间、成岩年龄缺少详细的年代学研究,本文在野外地质调查基础上,选取热水钼矿区似斑状黑云母二长花岗岩展开详细的岩石地球化学及年代学研究,首次对热水钼矿区似斑状黑云母二长花岗岩进行报道,同时结合前人研究成果初步探讨该岩石成因及动力学背景。

1 地质背景

热水钼多金属矿床位于中国大陆中央造山带西段——东昆仑造山带的东昆北构造带^[35],在祁漫塔格—都兰多金属成矿带、鄂拉山成矿亚带上,大

地构造位置处于西秦岭、柴达木北缘、东昆仑、巴颜喀拉4个地体交汇位置(图1-a)。区内岩浆活动频繁,以华力西-印支期岩浆岩活动最为频繁。

热水地区出露地层除第四系之外主要为古元古界金水口岩群,三叠系鄂拉山组的一套含火山物质的复理石建造和中酸性火山岩;其次为石炭系大干沟组、二叠系及少量新近系出露。

热水钼矿区出露地层主要有下石炭统大干沟组与第四系。矿区内断裂构造较发育,主要由一条区域性断裂及受其控制的3组断裂及破碎带,构成了矿区构造基本格架(图1-b)。矿区内岩浆活动十分强烈,主要以中酸性侵入岩为主,构成了矿区围岩主体,其岩性为二长花岗岩、花岗闪长岩以及似斑状黑云母二长花岗岩、花岗闪长斑岩,其中似斑状黑云母二长花岗岩为矿区矿(化)体的主要围岩。

2 样品采集及分析测试

所采样品为新鲜的似斑状黑云母二长花岗岩,风化面肉红色,新鲜面为淡肉红色调及灰白色,似斑状结构,块状构造,岩石中斑晶为钾长石,含量约15%,颗粒自形,粒径大小在8~12 mm,镜下鉴定斑晶大部分为微斜长石,可见格子双晶,晶体呈粒状,钾长石斑晶常由数个小晶体聚集而成,呈聚合变晶体,晶体内常有許多斜长石黑云母矿物小包裹体;基质为中细粒结构,主要由斜长石,碱性长石、石

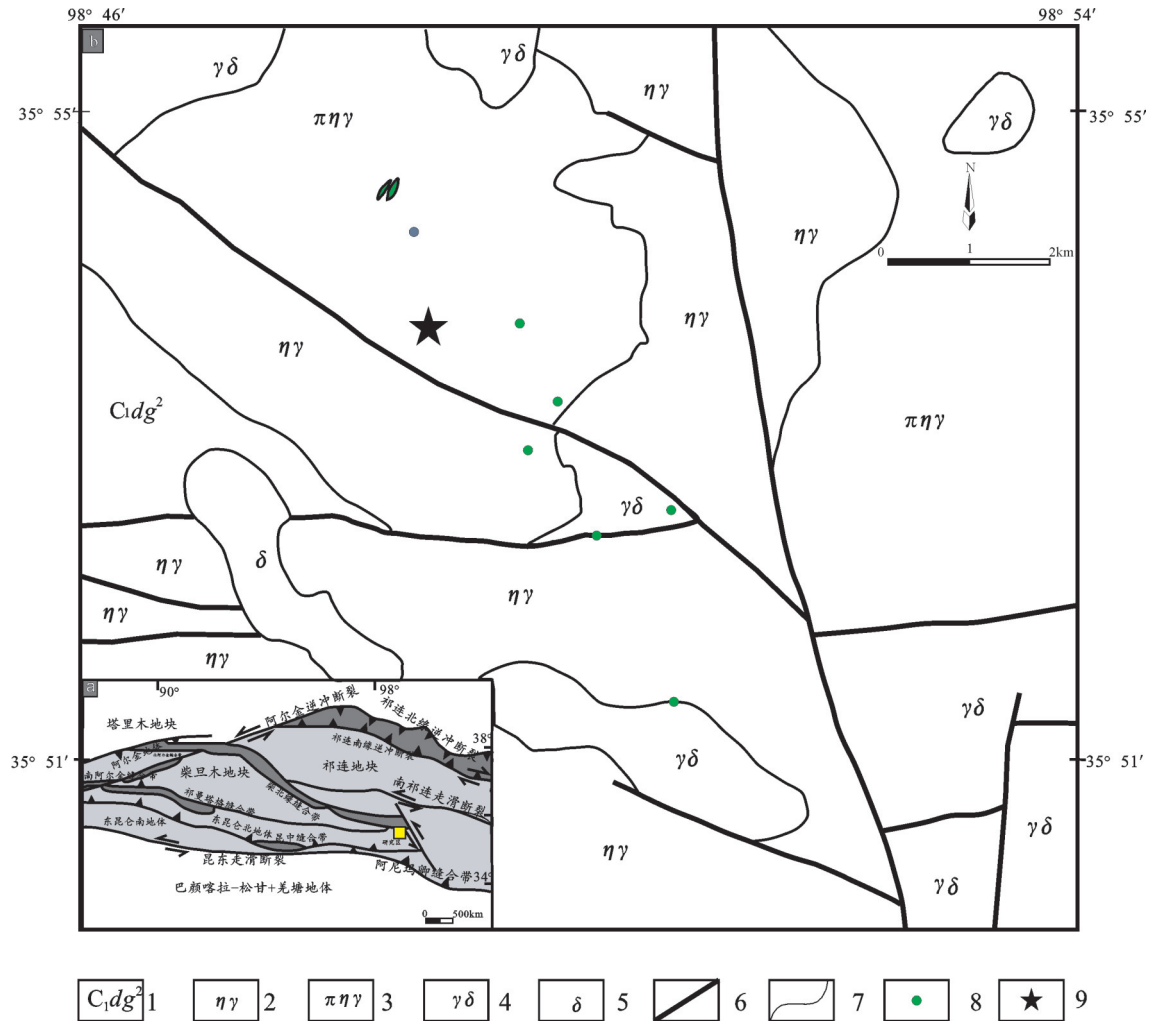


图1 热水铝多金属矿地质简图(图a据[36, 37]修改)
 1—石炭系酸性熔岩组:浅肉红色流纹岩及灰绿色薄层粉砂岩,细砂岩夹灰岩;2—灰白—肉红色二长花岗岩;3—灰白—肉红色似斑状黑云母二长花岗岩;4—灰白色花岗闪长岩;5—灰绿色闪长岩、角闪闪长岩;6—断层;7—地质界线;8—铜矿化点;9—采样位置

Fig.1 Geological sketch map of the Reshui Mo polymetallic ore district
 1—Carboniferous acidic lava group: light red rhyolite and celadon thin layer siltstone, fine sandstone with limestone; 2—Grayish white— red monzonitic granite; 3— Grayish white and red porphyritic monzonitic granite; 4— Grayish white granodiorite; 5—Diorite, hornblende diorite; 6— Fault; 7—Geological boundary; 8—Copper mineralized site; 9— Sampling location

英、黑云母组成,斜长石晶体呈粒状或板状,粒径大小0.5~2 mm,含量约30%,碱性长石种属为微斜长石,晶体呈粒状,粒径大小1.2~3.5 mm,含量约25%,石英晶体呈粒状或不规则粒状,粒径大小在0.5~3.5mm,波状消光,含量约25%,黑云母呈片状,粒径小于2 mm,常呈聚晶体出现,含量约5%(图2),含少量副矿物、磷灰石、锆石等。

此次样品主量元素、微量及稀土元素由中国地质调查局西安地质调查中心国土资源部岩浆作用成矿与找矿重点实验室进行地球化学分析。主量

元素样品进行熔融后分析,采用Magix_pro2440 X荧光光谱仪进行测定,微量元素(包括稀土元素)样品进行酸溶后分析,采用电感耦合等离子质谱法测定,仪器采用美国热电(ThermoElemental X7)ICP-MS。主量元素分析精度优于1%,微量和稀土元素分析精度控制在10%以内。

新鲜原岩锆石挑选由河北省廊坊区域地质调查所实验室完成。锆石阴极发光照相在西北大学大陆动力学国家重点实验室完成,LA-ICP-MS 锆石U-Th-Pb 同位素测定在西安地质调查中心国土

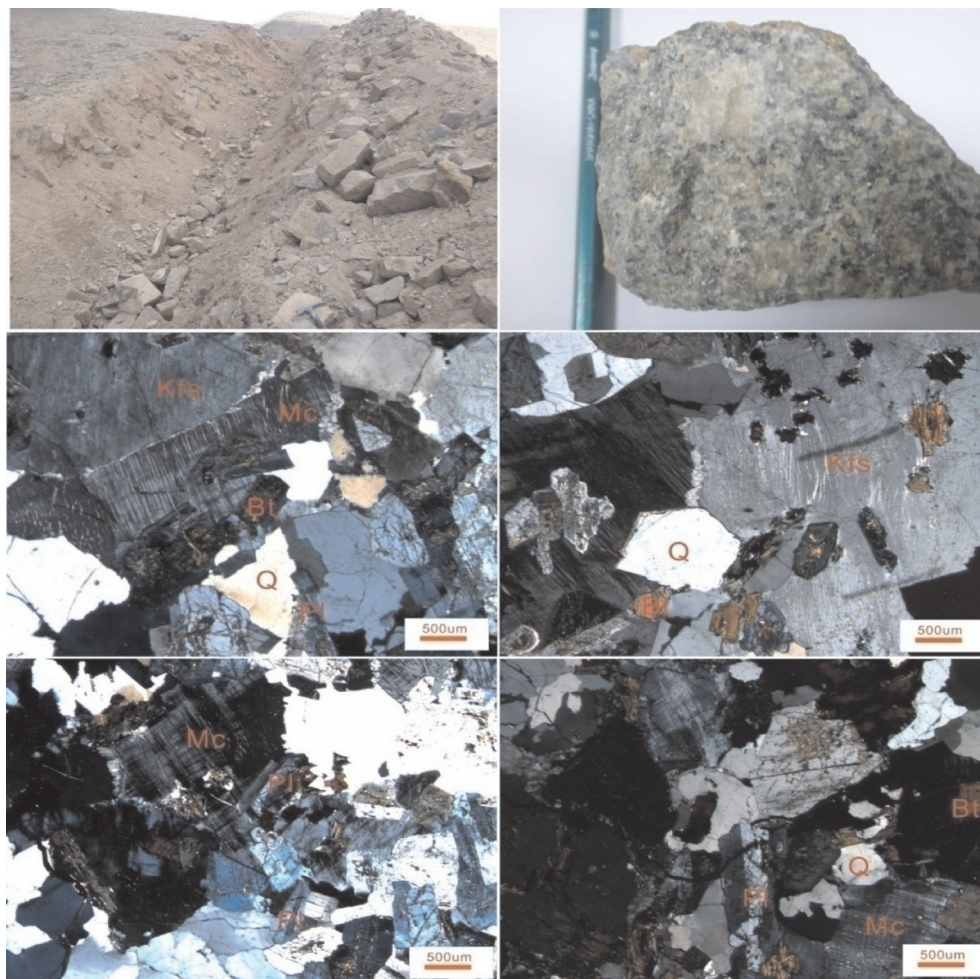


图2 热水似斑状黑云母二长花岗岩野外及镜下显微结构照片

Kfs—钾长石; Mc—微斜长石; Pl—斜长石; Bt—黑云母; Q—石英

Fig.2 Outcrop picture and microstructure photographs of porphyroid biotite monzogranite from the Reshui ore district

Kfs—K-feldspar; Mc—Microcline; Pl—Plagioclase; Bt—Biotite; Q—Quartz

资源部岩浆作用成矿与找矿重点实验室完成。分析在 Agilent 型 ICP-MS 和德国 Lambda Physik 公司的 ComPex 102 ArF 准分子激光器(工作物质 ArF, 波长 193 nm), 以及 MicroLas 公司的 GeoLas200 M 光学系统的联机上进行。激光剥蚀斑束直径为 30 μm , 激光剥蚀样品的深度为 20~40 μm 。实验中采用氦作为剥蚀物质的载气, 用美国国家标准技术研究院研制的人工合成硅酸盐玻璃标准参考物质 NISTSRM610 进行仪器最佳化标准, 锆石 U-Th-Pb 同位素组成分析以国际标准锆石 91500 作为外标标准物质, 元素含量采用 NIST SRM610 作为外标, ^{29}Si 作为内标, 采样方式为单点剥蚀, 数据采集选用 1 个质量峰 1 点的跳峰方式, 每完成 5 个测

点加测标样 1 次。在所测锆石样品分析 40 个点之前、后各测 1 次 NISTSRM 610, 具体实验操作及流程详参考文献[38], 锆石测定点的同位素比值、U-Pb 表面年龄和 U-Th-Pb 含量计算采用 GLITTER (Ver 4.0) 程序, 实验获得的数据采用 Andersen (2002) 方法进行同位素比值的校正, 以扣除普通 Pb 的影响。年龄计算采用国际标准程序 Isoplot(版本号 4.15)^[39], 采用年龄为 $^{206}\text{Pb}/^{238}\text{U}$ 年龄, 其加权平均值的误差为 1σ 。

3 测试结果

3.1 岩石地球化学特征

岩石地球化学成分见表 1 和表 2, 似斑状黑云母二

长花岗岩SiO₂含量在67.64%~71.09%,平均70.19%, Al₂O₃含量在13.8%~14.57%,平均14.22%,Na₂O含量在2.23%~3.02%,平均2.81%,K₂O含量在3.95%~5.18%,平均4.29%,K₂O/Na₂O值1.35~2.32,里特曼指数1.73~1.99,均值1.84,分异指数DI为75.57~82.62, Mg[#]值为39.11~55.81,铝饱和指数(A/CNK)除一件样品外,其余均大于1,平均为1.01,在SiO₂-K₂O图解中落入高钾钙碱性系列区域,岩石属于高钾钙碱性弱过铝岩石系列(图3)。

在微量元素蛛网图上岩石总体富集大离子亲

石元素Rb、Th、U、K、Pb等,明显亏损高场强元素Ta、Nb、Ce等,贫P、Ti(图4)。稀土元素总量(ΣREE)为94.27×10⁻⁶~127.44×10⁻⁶,平均为110.92×10⁻⁶,LREE/HREE为12.77~17.45,La_N/Yb_N为18.08~32.08,稀土元素配分曲线呈右倾型,具有较明显的轻稀土富集、重稀土亏损的特征,弱到中等程度的

表2 热水似斑状黑云母二长花岗岩微量元素(10⁻⁶)和稀土元素(10⁻⁶)

Table 2 Trace elements (10⁻⁶) and REE (10⁻⁶) of porphyroid biotite monzogranite

分析项目	14RSH01	14RSH02	14RSH03	14RSH04	14RSH05
Pb	29.00	26.00	24.40	32.60	24.70
Cr	10.80	8.64	7.56	4.38	5.73
Ni	3.46	2.83	4.04	1.83	2.35
Co	5.14	3.69	4.68	3.14	3.84
Cd	0.48	0.09	0.20	0.36	0.15
Li	22.70	16.90	17.20	18.10	17.20
Rb	223.00	134.00	106.00	126.00	130.00
Sr	241.00	252.00	189.00	261.00	238.00
Ba	584.00	501.00	366.00	720.00	452.00
V	23.40	21.80	23.60	18.30	20.40
Sc	5.36	6.48	6.03	8.37	7.22
Nb	15.60	11.60	14.80	14.50	13.50
Ta	1.12	0.84	1.00	1.21	0.94
Zr	148.00	140.00	132.00	146.00	156.00
Hf	4.64	3.98	3.86	4.40	4.48
Be	1.96	2.14	2.16	2.72	2.25
Ga	18.40	16.90	16.00	17.90	17.70
Sn	4.28	2.78	2.85	2.99	3.32
U	4.00	2.31	3.41	4.64	3.27
Th	19.50	16.30	16.30	20.80	16.20
La	30.50	33.10	21.50	22.90	24.50
Ce	56.10	60.20	41.20	42.60	47.10
Pr	6.44	6.85	4.79	4.61	5.31
Nd	20.30	22.20	16.00	14.50	17.30
Sm	4.17	4.20	3.38	3.03	3.08
Eu	0.83	0.82	0.70	0.72	0.68
Gd	3.14	2.94	2.52	2.14	2.19
Tb	0.44	0.39	0.34	0.29	0.28
Dy	2.30	1.86	1.75	1.54	1.48
Ho	0.43	0.32	0.32	0.29	0.26
Er	1.21	0.82	0.88	0.75	0.71
Tm	0.18	0.12	0.13	0.11	0.11
Yb	1.21	0.74	0.80	0.69	0.69
Lu	0.19	0.11	0.12	0.10	0.10
Y	11.70	8.64	9.14	7.93	7.60
ΣREE	127.44	134.67	94.43	94.27	103.79
LREE	118.34	127.37	87.57	88.36	97.97
HREE	9.10	7.30	6.86	5.91	5.82
LREE/HRE	13.00	17.45	12.77	14.95	16.83
La _N /Yb _N	18.08	32.08	19.28	23.81	25.47
δ Eu	0.70	0.71	0.73	0.86	0.80
δ Ce	0.98	0.98	1.00	1.02	1.01

表1 热水似斑状黑云母二长花岗岩主量元素(%)

Table 1 Major elements (%) of porphyroid biotite monzogranite

分析项目	14RSH01	14RSH02	14RSH03	14RSH04	14RSH05
SiO ₂	70.30	71.01	67.64	71.09	70.95
TiO ₂	0.30	0.30	0.32	0.31	0.31
Al ₂ O ₃	14.18	14.31	13.80	14.57	14.23
Fe ₂ O ₃	0.75	0.29	0.50	0.32	0.36
FeO	1.90	1.91	1.97	1.79	1.82
MnO	0.04	0.05	0.05	0.03	0.04
MgO	0.84	0.90	1.54	0.69	0.76
CaO	1.92	2.56	3.87	2.30	2.70
Na ₂ O	2.23	2.99	2.85	3.02	2.97
K ₂ O	5.18	4.05	3.95	4.27	4.02
P ₂ O ₅	0.08	0.08	0.09	0.08	0.08
灼失量	2.27	1.55	3.41	1.52	1.75
H ₂ O ⁺	0.49	0.54	0.90	0.83	0.81
Total	100.48	100.54	100.89	100.82	100.80
Q	31.98	30.69	26.43	30.75	30.95
An	9.21	12.37	13.66	11.06	13.10
Ab	19.31	25.70	24.97	25.95	25.58
Or	31.33	24.31	24.17	25.63	24.18
C	1.64	0.55	0.00	1.00	0.28
Di	0.00	0.00	4.59	0.00	0.00
Hy	4.65	5.19	4.58	4.35	4.58
Il	0.58	0.58	0.63	0.60	0.60
Mt	1.11	0.43	0.75	0.47	0.53
Ap	0.19	0.19	0.22	0.19	0.19
DI	82.62	80.70	75.57	82.33	80.71
SI	7.71	8.88	14.25	6.84	7.65
AR	2.71	2.43	2.25	2.52	2.41
σ43	1.99	1.76	1.83	1.88	1.73
R1	2661.00	2694.00	2582.00	2639.00	2711.00
R2	538.00	609.00	788.00	575.00	617.00
Mg [#]	40.33	44.26	55.81	39.11	40.84
A/NKC	1.11	1.02	0.86	1.06	1.00
A/NK	1.53	1.54	1.54	1.52	1.54

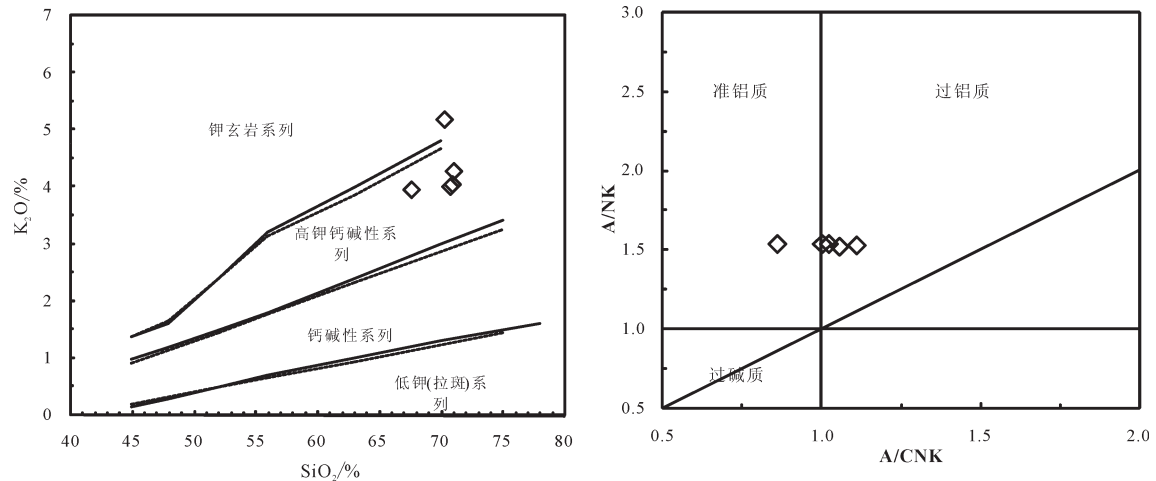


图3 似斑状黑云母二长花岗岩的 $\text{SiO}_2\text{-K}_2\text{O}$ (a)^[40]和 A/CNK-A/NK (b)图解^[41]
Fig.3 $\text{SiO}_2\text{-K}_2\text{O}$ (a)^[40] and A/CNK-A/NK (b)^[41] diagrams of porphyroid biotite monzogranite

负锶异常(图5)。

3.2 锆石LA-ICP-MS定年结果

本文对热水矿区出露的似斑状黑云母二长花岗岩展开锆石年代学研究,样品中锆石粒径长45~260 μm ,长宽比介于2:1~5:1,多呈长柱状,自形程度较高,绝大多数锆石具有清晰的振荡环带结构(图6),显示它属于岩浆的结晶产物。锆石Th/U比值为0.43~1.98,均大于0.4,显示出它属于岩浆锆石成因特征^[44-46]。

对样品的U-Pb分析测试而得到的同位素比值和年龄数据见表3,本次共分析测试了30个点,这些测点位于振荡环带上,其中6个测点信号不好,在年龄计算时剔除,对剩余24个测点数据进行了U-Pb年龄谐和投图及加权平均年龄计算,结果显示,这些测点数据均位于或接近U-Pb谐和线(图7),其中 $^{206}\text{Pb}/^{238}\text{U}$ 表面年龄介于230~232 Ma(表3),表明锆石在形成之后U-Pb体系是封闭的,基本上没有明显的U或Pb的加入或丢失。 $^{206}\text{Pb}/^{238}\text{U}$ 加权平均年龄为(230.9±1.4) Ma(MSWD=0.020)(图7),代表岩石的结晶年龄。因此热水铀矿区似斑状黑云母二长花岗岩年龄为(230.9±1.4) Ma,即其成岩时代在晚三叠世。

4 讨论

4.1 成岩年龄及其意义

热水铀矿区似斑状黑云母二长花岗岩成岩年

龄(230.9±1.4) Ma(MSWD=0.020),为印支期,其形成时代为三叠世晚期,表明为三叠世岩浆活动的产物。已有大量研究表明(表4),热水地区普遍存在印支期花岗岩浆及成矿事件,该地区哈陇休玛钨钼矿化(体)岩体花岗闪长斑岩锆石U-Pb年龄为(230±1) Ma^[34];哈日扎铜多金属矿花岗闪长斑岩形成时代为(234.5±4.8) Ma^[33];什多龙钨铅锌矿辉钼矿Re-Os年龄为(236.2±2.1) Ma^[47];双庆沟铁铅锌多金属矿两件斜长花岗岩LA-ICP-MS锆石U-Pb年龄分别为(227.2±1.0) Ma、(226.54±0.97) Ma,辉钼矿Re-Os年龄为(226.5±5.1) Ma^[48],本文定年结果与该地区所属的东昆仑鄂拉山成矿亚带成岩成矿年龄一致,区域地质资料显示,鄂拉山岩浆带侵入体年龄值基本上均落入195~231 Ma^[49],因而该岩体与鄂拉山岩浆岩带有密切关系。

4.2 岩石成因及源区性质

热水铀矿区似斑状黑云母二长花岗岩由岩石地球化学特征可知,岩石中 SiO_2 含量大于66%,属于酸性岩石类型,其中14RSHX03样品可能受到蚀变影响,其 $\text{SiO}_2\text{-Al}_2\text{O}_3$ 含量较其他样品低,CaO含量较其他样品含量高,与哈日扎花岗闪长斑岩,哈陇休玛花岗闪长斑岩具有相似的地球化学特征^[33, 34],均为高钾钙碱性岩石。Frost^[50]将 $\text{FeO}^{\text{T}}/(\text{FeO}^{\text{T}}+\text{MgO})$ 定义为Fe原子数,将 $\text{Na}_2\text{O}+\text{K}_2\text{O}-\text{CaO}$ 定义为钙碱指数,用以区别A型、S型、I型3种花岗岩,根据 $\text{SiO}_2\text{-FeO}^{\text{T}}/(\text{FeO}^{\text{T}}+\text{MgO})$ 图解(图8),热水似斑状黑云母二

表3 似斑状黑云母二长花岗岩 LA-ICP-MS 锆石 U-Th-Pb 同位素测试结果

Table 3 LA-ICP-MS zircon U-Th-Pb isotope analytical results of porphyroid biotite monzogranite

测点号	Th/ 10^{-6}	U/ 10^{-6}	Th/U	同位素比值						表面年龄 /Ma					
				$^{207}\text{Pb}/^{206}\text{Pb}$	1 σ	$^{207}\text{Pb}/^{235}\text{U}$	1 σ	$^{206}\text{Pb}/^{238}\text{U}$	1 σ	$^{207}\text{Pb}/^{206}\text{Pb}$	1 σ	$^{207}\text{Pb}/^{235}\text{U}$	1 σ	$^{206}\text{Pb}/^{238}\text{U}$	1 σ
004R101	258.04	435.37	0.59	0.05162	0.00194	0.25981	0.0098	0.0365	0.00057	268.6	83.91	234.5	7.9	231.1	3.54
005R102	365.94	771.04	0.47	0.05154	0.00147	0.2596	0.00758	0.03653	0.00053	265.2	64.28	234.3	6.11	231.3	3.32
006R103	302.49	333.51	0.91	0.05664	0.00497	0.28553	0.02452	0.03656	0.00089	476.9	183.72	255	19.37	231.5	5.56
007R104	262.73	567.80	0.46	0.05656	0.00184	0.28522	0.00936	0.03657	0.00055	473.6	71.07	254.8	7.4	231.6	3.45
008R105	90.49	167.67	0.54	0.05119	0.00252	0.25663	0.01254	0.03636	0.00062	249.2	109.35	231.9	10.14	230.2	3.83
010R106	372.98	655.46	0.57	0.05215	0.00185	0.26256	0.00938	0.03651	0.00056	292	78.98	236.7	7.54	231.2	3.49
011R107	594.25	855.78	0.69	0.05062	0.00164	0.25476	0.00834	0.0365	0.00055	223.6	73.13	230.4	6.75	231.1	3.4
012R108	147.73	216.70	0.68	0.05264	0.0028	0.26389	0.01391	0.03636	0.00065	313.1	116.63	237.8	11.18	230.2	4.01
013R109	446.94	992.64	0.45	0.04966	0.00182	0.25011	0.00918	0.03652	0.00056	179.1	83.05	226.7	7.46	231.3	3.51
014R110	404.67	477.21	0.85	0.05055	0.00224	0.25479	0.01122	0.03655	0.0006	220.5	99.2	230.5	9.08	231.4	3.72
018R111	286.15	555.49	0.52	0.05807	0.00183	0.29259	0.00934	0.03654	0.00055	531.8	68.14	260.6	7.34	231.4	3.42
020R113	583.91	294.38	1.98	0.04863	0.00376	0.24571	0.01871	0.03664	0.00079	130.2	172.59	223.1	15.25	232	4.89
021R114	99.88	234.86	0.43	0.04904	0.00202	0.24621	0.01015	0.03641	0.00058	149.8	93.99	223.5	8.27	230.5	3.61
022R115	348.44	586.31	0.59	0.05406	0.002	0.27202	0.01011	0.03649	0.00057	373.4	81.19	244.3	8.07	231	3.54
024R116	424.99	753.89	0.56	0.05087	0.00168	0.25567	0.00851	0.03645	0.00055	234.9	74.28	231.2	6.88	230.8	3.4
026R118	312.03	568.24	0.55	0.05138	0.00216	0.25787	0.01081	0.03639	0.00059	257.9	93.73	232.9	8.73	230.4	3.65
028R120	348.35	694.03	0.50	0.05163	0.00142	0.25912	0.0073	0.03639	0.00052	269.1	61.7	234	5.88	230.4	3.26
032R121	460.93	782.39	0.59	0.05319	0.00166	0.26645	0.00845	0.03633	0.00054	336.8	69.37	239.9	6.77	230	3.36
033R122	410.45	584.41	0.70	0.05174	0.00186	0.25949	0.00939	0.03637	0.00056	273.9	80.37	234.3	7.57	230.3	3.48
034R123	588.95	666.80	0.88	0.0498	0.00132	0.25084	0.00685	0.03653	0.00052	185.5	60.56	227.3	5.56	231.3	3.24
035R124	512.74	649.23	0.79	0.05202	0.00187	0.26094	0.00943	0.03638	0.00056	286.1	80.11	235.4	7.6	230.3	3.48
036R125	200.41	523.81	0.38	0.05196	0.00191	0.2608	0.00962	0.0364	0.00056	283.5	81.78	235.3	7.74	230.5	3.49
040R128	258.92	581.88	0.44	0.0505	0.00174	0.25386	0.00882	0.03645	0.00055	218.1	77.92	229.7	7.14	230.8	3.43
041R129	301.56	687.76	0.44	0.05195	0.00152	0.26112	0.0078	0.03644	0.00053	283.4	65.6	235.6	6.28	230.8	3.3

长花岗岩投入镁质I型与S型花岗岩交汇区,在 SiO_2 - $(\text{Na}_2\text{O}+\text{K}_2\text{O}-\text{CaO})$ 图解中落在钙碱性I型花岗岩区域,结合岩相学观察,似斑状黑云母二长花岗岩中可见普通角闪石,因此根据地球化学特征及岩石矿物组成认为该岩石具有I型花岗岩特征。

Pitcher^[51]认为钙碱性I型花岗岩大量出现在与板块俯冲过程相关的陆缘弧中,热水似斑状黑云母二长花岗岩微量元素Ta, Yb值较低,具有亲弧特性^[52],La/Yb值高,说明下地壳物质局部熔融^[53]或岩浆的俯冲洋壳局部熔融^[54];岩石富集大离子亲石元素Rb、Th、U、K等,明显亏损高场强元素Ta、Nb、Ce等,其地球化学特征与弧火山岩具有相似特点,很

可能形成于加厚地壳背景下与板片俯冲有关的岛弧环境^[55];Mg[#]介于39.11~55.81,而下地壳岩石部分熔融形成的熔体其Mg[#]小于45^[56],在 SiO_2 -Mg[#]图解(图9)中落入埃达克质岩区域,可以看出似斑状黑云母二长花岗岩不为单纯的下地壳熔融来源,与Defant et al.定义的埃达克岩特征具有低Y、Yb,高Sr/Y和La/Yb的地球化学特征一致,进一步说明似斑状二长花岗岩的埃达克岩亲和性。Nb/Ta=11.98~14.8,介于地壳平均值12.5~13.5^[57]与地幔平均值17.5^[58]之间,反映具有壳幔混合成因特点。

综上认为似斑状黑云母二长花岗岩有埃达克岩亲和性,岩石为高钾钙碱性I型花岗岩,具有壳幔

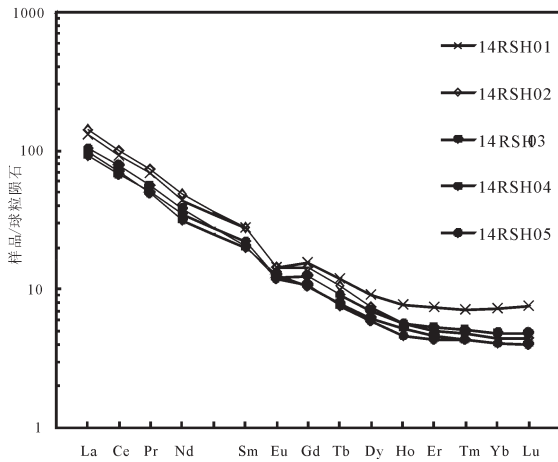


图4 似斑状黑云母二长花岗岩稀土元素配分模式图
(球粒隕石标准化值据[42])

Fig.4 Chondrite-normalized REE patterns of porphyroid biotite monzogranite

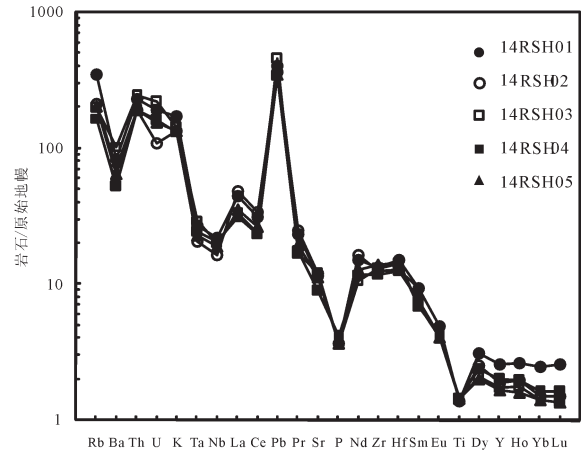


图5 似斑状黑云母二长花岗岩微量元素蛛网图
(原始地幔标准化值据[43])

Fig.5 Primitive mantle-normalized trace element spider diagrams of porphyroid biotite monzogranite

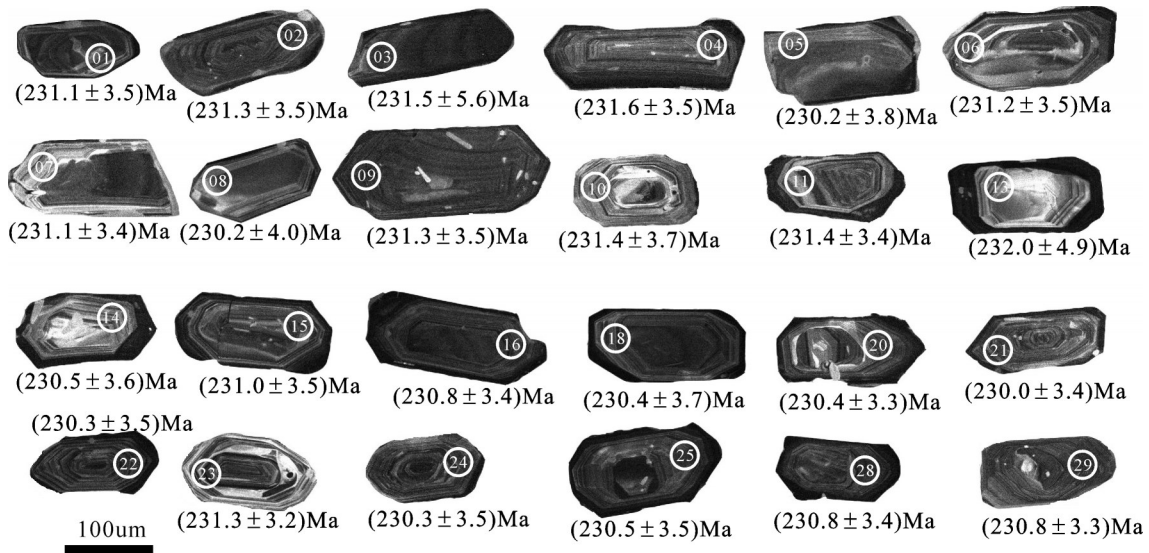


图6 似斑状黑云母二长花岗岩锆石CL图像

Fig.6 CL images of zircons from porphyroid biotite monzogranite

混合成因特点,形成陆缘弧环境中。

4.3 成岩动力学背景

高钾钙碱性I型花岗岩岩浆通常是由镁铁质-安山质火成岩派生出的高钾钙碱性火成岩部分熔融所产生,而这些源区中基性物质可能来源于富集次大陆的岩石圈地幔^[61],产生的机制通常为挤压向伸展体制转换,减压熔融作用使得地幔上涌,幔源物质上侵,为地壳提供了大量热源及物质,使得地壳中镁铁质-安山质钙碱性变火成岩部分熔融,产生高钾钙碱性熔浆,初步形成含矿的花岗质岩浆。

在该地区花岗岩中多可见镁铁质闪长岩包体^[3],说明有地幔物质的参与,东昆仑地区中-晚二叠世至三叠世(240~260 Ma)是主要的俯冲造山期^[62],在中晚三叠世时期,阿尼玛卿古特提斯洋闭合,地体开始碰撞^[63],该时期东昆仑正好处在大洋板块大规模俯冲碰撞阶段,火成岩具安第斯型活动大陆边缘构造属性^[64]。热水所属东昆仑造山带的鄂拉山成矿亚带,孙延贵(2004)认为鄂拉山经历了初始伸展期(361.5~393.5 Ma)、俯冲碰撞(开始:261.8~263.9 Ma)、碰撞造山(集中:200~220 Ma)以及造

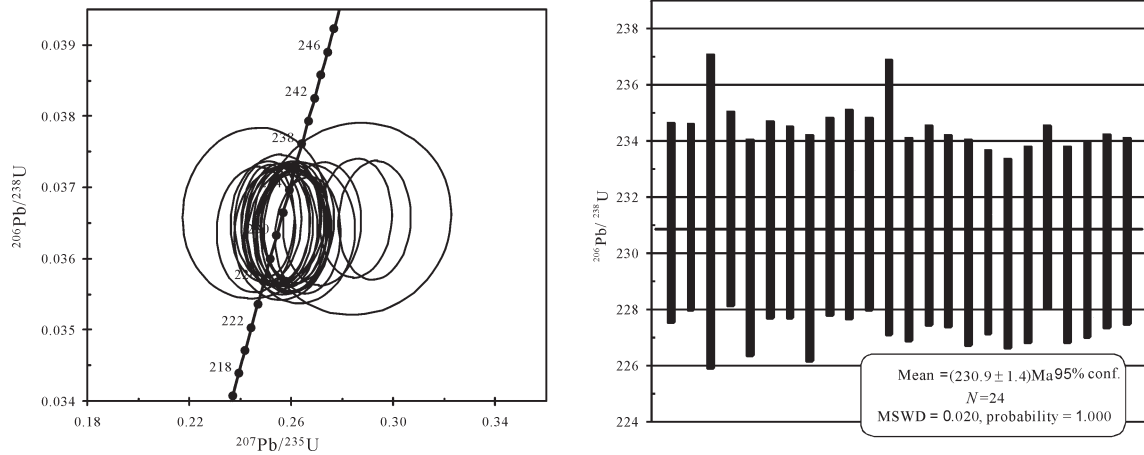


图7 似斑状黑云母二长花岗岩锆石U-Pb谐和图和加权平均年龄

Fig.7 Zircon U-Pb concordia diagram and histograms of weighted average ages of porphyroid biotite monzogranite

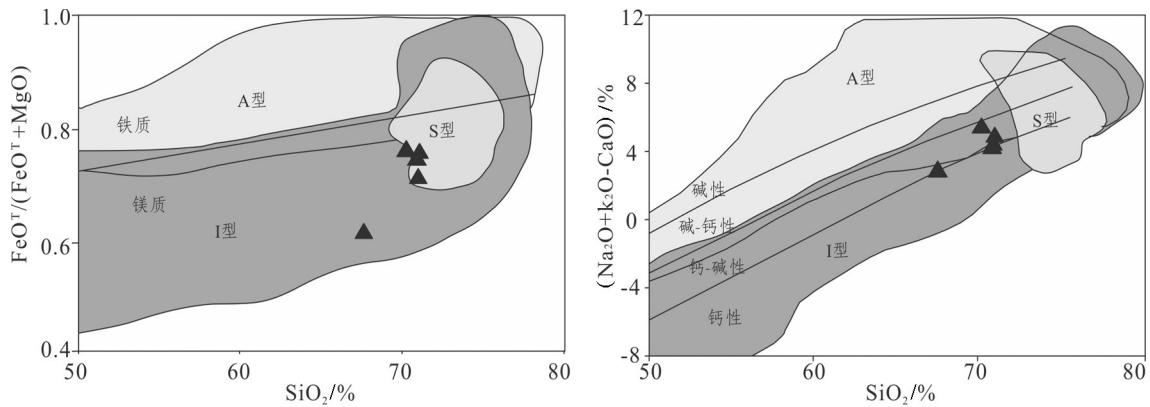


图8 似斑状黑云母二长花岗岩岩石类型判别图(底图据[50])

Fig.8 Porphyroid biotite monzogranite type discrimination diagram of the Reshui ore district (after[50])

表4 热水地区印支期含矿岩体(矿床)年龄及测试方法

Table 4 Age of Indosinian ore-bearing rock mass and testing method

地区	热水	哈日扎	哈龙休玛	什多龙	双庆沟	双庆沟
矿种	Mo、Cu、Pb、Zn、Ag	Cu、Pb、Zn	W、Mo	Pb、Zn	Pb、Zn	Pb、Zn
岩性	似斑状黑云母二长花岗岩	花岗闪长斑岩	花岗闪长斑岩	辉钼矿	辉钼矿	花岗岩
测试方法	LA-ICP-MS 锆石 U-Pb	LA-ICP-MS 锆石 U-Pb	LA-ICP-MS 锆石 U-Pb	Re-Os	Re-Os	LA-ICP-MS 锆石 U-Pb
形成时代/Ma	230.9±1.4	234.5±4.8	230±1	236.2±2.1	226.5 ± 5.1	227.2 ± 1.0、226.54 ± 0.97
资料来源	本文	[33]	[34]	[47]	[48]	[48]

山期后伸展垮塌(195.7~199.6 Ma)等构造事件^[65],热水似斑状黑云母二长花岗岩成岩年龄为(230.9±1.4)Ma,处于板块构造体制向陆内构造体制转变阶段,碰撞过程中加厚下地壳部分熔融,发生壳幔岩浆混合作用,为幔源物质参与该地区岩浆活动与

成矿作用提供了物质和能量基础。在该区已发现了哈龙休玛钨钼矿、哈日扎铜多金属矿,尽管哈日扎矿床存在争议,但毋庸置疑的是在该地区具有形成斑岩型矿床的潜力。因此初步认为热水钼多金属矿形成于构造体制转换阶段,下地壳物质部分熔

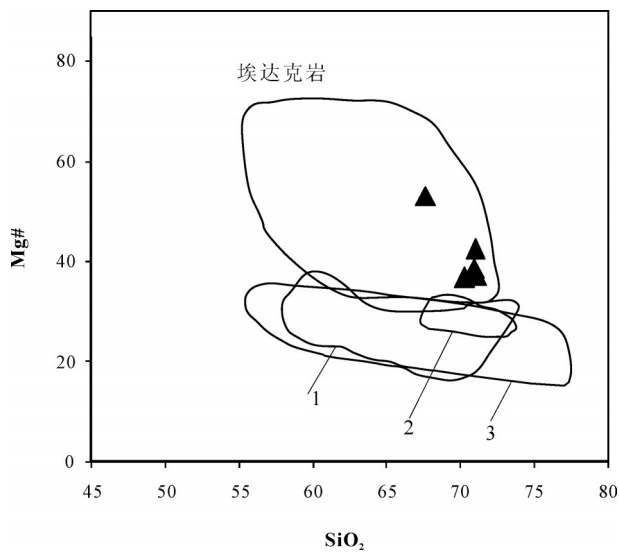


图9似斑状黑云母二长花岗岩 SiO_2 -Mg#图
1—压力7 kbar, 温度:825~950°C环境下纯地壳的局部熔融(据文献[59]);2—压力7~13 kbar, 温度:825~950°C环境下纯地壳的局部熔融(据文献[60]);3—压力8~16 kbar, 温度1000~1050°C环境下纯地壳的局部熔融(据文献[56])

Fig.9 Porphyroid biotite monzogranite of SiO_2 -Mg# diagram
1—Pure crustal partial melt at 7kbar and 825~950°C (after reference [59]); 1—Pure crustal partial melt at 7~13 kbar and 825~950°C (after reference [60]); 3—Pure crustal partial melt at 8~16kbar and 1000~1050°C (after reference [56])

融,幔源物质混入,初步形成了富矿的岩浆,在后期侵入过程中,岩浆多期次活动,物理化学条件发生变化,伴随构造运动,在适宜位置富矿物质得以沉淀,形成钼多金属矿。

5 结 论

通过对热水钼多金属矿似斑状黑云母二长花岗岩岩相学、岩石地球化学特征以及LA-ICP-MS锆石U-Pb年代学的研究,得出以下结论:

(1)似斑状黑云母二长花岗岩LA-ICP-MS锆石U-Pb年龄为 $(230.9 \pm 1.4)\text{Ma}$ (MSWD=0.020),其形成时代为晚三叠世,与区域上岩浆活动一致。

(2)似斑状黑云母二长花岗岩属于高钾钙碱性I型花岗岩,具有壳幔混合成因特点,形成于陆缘弧环境。

(3)似斑状黑云母二长花岗岩形成于构造体制转换阶段动力学背景,该地区具有形成斑岩型矿床潜力。

致谢:感谢项目组成员在野外的协助,西北大学大陆重点实验室以及中国地质调查局西安地质调查中心国土资源部岩浆作用成矿与找矿重点实验室工作人员在实验及测试上的指导与支持,在此一并感谢。

参考文献(References):

- [1] 袁万明, 莫宣学, 喻学惠, 等. 东昆仑印支期区域构造背景的花岗岩记录[J]. 地质论评, 2000, 46(2): 203-211.
Yuan Wanming, Mo Xuanxue, Yu Xuehui, et al. The record of Indosinian tectonic setting from the granitoid of Eastern Kunlun Mountains[J]. Geological Review, 2000, 46 (2): 203- 211(in Chinese with English abstract).
- [2] 姜春发. 中央造山带几个重要地质问题及其研究进展(代序)[J]. 地质通报, 2002, 21(8): 453-455.
Jiang Chunfa. Several important geological problems of central orogenic belt and its research progress [J]. Geological Bulletin of China, 2002, 21(8): 453-455 (in Chinese with English abstract).
- [3] 刘成东. 东昆仑造山带东段花岗岩岩浆混合作用[M]. 北京:地质出版社, 2008.
Liu Chengdong. East Section of East Kunlun Orogenic Belt Granite Magma Mingling [M]. Beijing:Geological Publishing House, 2008 (in Chinese with English abstract).
- [4] 杜玉良, 贾群子, 韩生福. 青海东昆仑成矿带中生代构造-岩浆-成矿作用及铜金多金属找矿研究[J]. 西北地质, 2012, 45(4):69-75.
Du Yuliang, Jia Qunzi, Han Shengfu. Mesozoic tectono-magmatic- mineralization and copper- gold polymetallic ore prospecting research in east Kunlun Metallogenic Belt in Qinghai [J]. Northwestern Geology, 2012, 45(4): 69- 75 (in Chinese with English abstract).
- [5] 丰成友, 李东生, 吴正寿, 等. 东昆仑祁漫塔格成矿带矿床类型、时空分布及多金属成矿作用[J]. 西北地质, 2010, 43(4): 10-17.
Feng Chengyou, Li Dongsheng, Wu Zhengshou, et al. Major types, time- space distribution and metallogenesis of polymetallic deposits in the Qimantag Metallogenic Belt, Eastern Kunlun area[J]. Northwestern Geology, 2010, 43(4): 10- 17 (in Chinese with English abstract).
- [6] 丰成友, 赵一鸣, 李大新, 等. 青海西部祁漫塔格地区矽卡岩型铁铜多金属矿床的矽卡岩类型和矿物学特征[J]. 地质学报, 2011, 85(7): 1108-1115.
Feng Chengyou, Zhao Yiming, Li Daxin, et al. Skarn types and mineralogical characteristics of the Fe- Cu- polymetallic skarn deposits in the Qimantag area, Western Qinghai Province[J]. Acta Geologica Sinica, 2011, 85(7): 1108- 1115 (in Chinese with English abstract).
- [7] 伍跃中, 乔耿彪, 陈登辉. 东昆仑祁漫塔格地区构造岩浆作用与成矿关系初步探讨[J]. 大地构造与成矿学, 2011, 25(2): 232-241.
Wu Yuezhong, Qiao Gengbiao, Chen Denghui. A preliminary study on relationship between tectonic magmatism and mineralization in Qimantag area, Eastern Kunlun Mountains[J]. Geotectonica et Metallogenia, 2011, 35(2): 232- 241(in Chinese with English

- abstract).
- [8] 武明德. 青海省东昆仑燕山期斑岩型矿床成矿潜力研究[D]. 中国地质大学(北京), 2013.
Wu Mingde. Ore Potential of the Yanshanian Porphyry Deposit, East Kunlun of Qinghai Province[D]. China University of Geosciences (Beijing), 2013(in Chinese with English abstract).
- [9] 许长坤, 刘世宝, 赵子基, 等. 青海省东昆仑成矿带铁矿成矿规律与找矿方向研究[J]. 地质学报, 2012, 86(10): 1621–1636.
Xu Changkun, Liu Shibao, Zhao Ziji, et al. Metallogenic law and prospect direction of iron deposits in the East Kunlun Metallogenic Belt in Qinghai[J]. Acta Geologica Sinica, 2012, 86(10): 1621–1636 (in Chinese with English abstract).
- [10] 赵财胜. 青海东昆仑造山带金、银成矿作用[D]. 长春: 吉林大学, 2004.
Zhao Caisheng. Gold, Silver Metallogeny in Eastern Kunlun Orogenic Belt, Qinghai Province[D]. Changchun: Jilin University, 2004(in Chinese with English abstract).
- [11] 赵俊伟. 青海东昆仑造山带造山型金矿床成矿系列研究[D]. 长春: 吉林大学, 2008.
Zhao Junwei. Study on Orogenic Gold Metallogenic Series in Eastern Kunlun Orogenic Belt, Qinghai Province[D]. Changchun: Jilin University, 2008(in Chinese with English abstract).
- [12] 张文秦. 青海省东昆仑地区火成岩的岩石-地球化学基本特征及含矿性研究[D]. 中国地质大学(北京), 2003.
Zhang Wenqin. The East Kunlun Area of Igneous Rock – Geochemical Characteristics and Ore Research, Qinghai Province[D]. China University of Geosciences (Beijing), 2003 (in Chinese with English abstract).
- [13] 张德全, 丰成友, 李大新, 等. 柴北缘—东昆仑地区的造山型金矿床[J]. 矿床地质, 2001, 20(2): 137–146.
Zhang Dequan, Feng Chengyou, Li Daxin, et al. Orogenic gold deposits in the North Qaidam and East Kunlun Orogen, West China[J]. Mineral Deposits, 2001, 20(2): 137–146(in Chinese with English abstract).
- [14] 胡正国, 刘继庆, 钱壮志, 等. 东昆仑区域成矿规律初步研究[J]. 黄金科学技术, 1998, 6(5): 6–13.
Hu Zhengguo, Liu Jiqing, Qian Zhuangzhi, et al. A study of the regional metallogenetic regularity in East Kunlun Mountain[J]. Gold Science and Technology, 1998, 6(5): 6–13(in Chinese with English abstract).
- [15] 罗照华, 柯珊, 曹永清, 等. 东昆仑印支晚期幔源岩浆活动[J]. 地质通报, 2002, 21(6): 292–297.
Luo Zhaohua, Ke Shan, Cao Yongqing, et al. Late Indosinian mantle-derived magmatism in the East Kunlun[J]. Geological Bulletin of China, 2002, 21(6): 292–297 (in Chinese with English abstract).
- [16] 王松, 丰成友, 李世金, 等. 青海祁漫塔格卡尔却卡铜多金属矿区花岗闪长岩锆石 SHRIMP U–Pb 测年及其地质意义[J]. 中国地质, 2009, 36(1): 74–84.
Wang Song, Feng Chengyou, Li Shijin, et al. Zircon SHRIMP U–Pb dating of granodiorite in the Kaerqueka polymetallic ore deposit, Qimantag Mountain, Qinghai Province, and its geological implications[J]. Geology in China, 2009, 36(1): 74–84 (in Chinese with English abstract).
- [17] 苏旭亮, 赵永亮, 赵闯, 等. 东昆仑祁漫塔格克停哈尔斑岩型铜矿找矿突破思路及找矿模型[J]. 中国地质, 2014, 41(6): 2048–2062.
Su Xuliang, Zhao Yongliang, Zhao Chuang, et al. Prospecting thinking and model for the Ketinghaer porphyry copper molybdenum deposit in the East Kunlun Mountains[J]. Geology in China, 2014, 41(6): 2048–2062(in Chinese with English abstract).
- [18] 刘建楠, 丰成友, 元锋, 等. 青海都兰县下得波利铜钼矿区锆石 U–Pb 测年及流体包裹体研究[J]. 岩石学报, 2012, 28(2): 679–690.
Liu Jiannan, Feng Chengyou, Qi Feng, et al. SIMS zircon U–Pb dating and fluid inclusion studies of Xiadeboli Cu–Mo ore district in Dulan County, Qinghai Province, China[J]. Acta Petrologica Sinica, 2012, 28(2): 679–690. (in Chinese with English abstract).
- [19] 丰成友, 王松, 李国臣, 等. 青海祁漫塔格中晚三叠世花岗岩: 年代学、地球化学及成矿意义[J]. 岩石学报, 2012, 28(2): 665–678.
Feng Chengyou, Wang Song, Li Guocheng, et al. Middle to Late Triassic granitoids in the Qimantag area, Qinghai Province, China: Chronology, geochemistry and metallogenic significances[J]. Acta Petrologica Sinica, 2012, 28(2): 665–678 (in Chinese with English abstract).
- [20] 姜常义, 凌锦兰, 周伟, 等. 东昆仑夏日哈木镁铁质—超镁铁质岩体岩石成因与拉张型岛弧背景[J]. 岩石学报, 2015, 31(4): 1117–1136.
Jiang Changyi, Lin Jinlan, Zhou Wei, et al. Petrogenesis of the Xiarihamu Nibearing layered mafic–ultramafic intrusion, East Kunlun: Implications for its extensional island arc environment[J]. Acta Petrologica Sinica, 2015, 31(4): 1117–1136(in Chinese with English abstract).
- [21] 杨延乾, 李碧乐, 许庆林, 等. 东昆仑埃坑德勒斯特二长花岗岩锆石 U–Pb 定年及地质意义[J]. 西北地质, 2013, 46(1): 56–62.
Yang Yanqian, Li Bile, Xu Qinglin, et al. Zircon U–Pb ages and its geological significance of the monzonitic granite in the Aikengdelesite, Eastern Kunlun[J]. Northwestern Geology, 2013, 46(1): 56–62(in Chinese with English abstract).
- [22] 奚仁刚, 校培喜, 伍跃中, 等. 东昆仑肯德可克铁矿区二长花岗岩组成、年龄及地质意义[J]. 西北地质, 2010, 43(4): 195–202.
Xi Rengang, Xiao Peixi, Wu Yuezhong, et al. The geological significances, composition and age of the monzonitic granite in Kendekeke Iron Mine[J]. Northwestern Geology, 2010, 43(4): 195–202(in Chinese with English abstract).
- [23] 奥琮, 孙丰月, 李碧乐, 等. 青海夏日哈木矿区中泥盆世闪长玢岩锆石 U–Pb 年代学、地球化学及其地质意义[J]. 西北地质, 2014, 47(1): 96–106.
Ao Cong, Sun Fengyue, Li Bile, et al. Geochemistry, Zircon U–Pb dating and geological significance of diorite porphyrite in Xiarihamu Deposit, Eastern Kunlun Orogenic Belt, Qinghai[J]. Northwestern Geology, 2014, 47(1): 96–106(in Chinese with English abstract).
- [24] 杨延乾, 李碧乐, 许庆林, 等. 东昆仑埃坑德勒斯特二长花岗岩锆石 U–Pb 定年及地质意义[J]. 西北地质, 2013, 46(1): 56–62.
Yang Yanqian, Li Bile, Xu Qinglin, et al. Zircon U–Pb ages and

- its geological significance of the monzonitic granite in the Aikengdelesite, Eastern Kunlun[J]. *Northwestern Geology*, 2013, 46(01): 56–62(in Chinese with English abstract).
- [25] 高永宝, 李文渊, 马晓光, 等. 东昆仑杂林格铁矿床成因年代学及Hf同位素制约[J]. *兰州大学学报(自然科学版)*, 2012, 48(2): 36–47.
- Gao Yongbao, Li Wenyuan, Ma Xiaoguang, et al. Genesis, geochronology and Hf isotopic compositions of the magmatic rocks in Galinge iron deposit, Eastern Kunlun[J]. *Journal of Lanzhou University (Natural Sciences)* 2012, 48(2): 36–47 (in Chinese with English abstract).
- [26] 赵财胜, 杨富全, 代军治. 青海东昆仑肯德可克钴铋金矿床成因年龄及意义[J]. *矿床地质*, 2006,(S1):427–430.
- Zhao Caisheng, Yang Fuquan, Dai Junzhi. Metallogenic age of the Kendekeke Co, Bi, Au deposit in East Kunlun Mountains, Qinghai Province, and its significance[J]. *Mineral Deposits*, 2006, (S1): 427–430(in Chinese with English abstract).
- [27] 肖晔, 丰成友, 刘建楠, 等. 青海肯德可克铁多金属矿区年代学及硫同位素特征[J]. *矿床地质*, 2013,32(01):177–186.
- Xiao Ye, Feng Chengyou, Liu Jiannan, et al. LA–MC–ICP–MS zircon U–Pb dating and sulfur isotope characteristics of Kendekeke Fe– polymetallic deposit, Qinghai Province[J]. *Mineral Deposits*, 2013, 32(01): 177–186(in Chinese with English abstract).
- [28] 丰成友, 王雪萍, 舒晓峰, 等. 青海祁漫塔格虎头崖铅锌多金属矿区年代学研究及地质意义[J]. *吉林大学学报(地球科学版)*, 2011,41(6):1806–1817.
- Feng Chengyou, Wang Xueping, Shu Xiaofeng, et al. Isotopic chronology of the Hutouya skarn lead–zinc polymetallic ore district in Qimantag area of Qinghai Province and its geological significance [J].*Journal of Jilin University(Earth Science Edition)*, 2011,41(6):1806–1817 (in Chinese with English abstract).
- [29] 李世金, 孙丰月, 丰成友, 等. 青海东昆仑鸭子沟多金属矿的成因年代学研究[J]. *地质学报*, 2008, 82(7): 949–955.
- Li Shijin, Sun Fengyue, Feng Chengyou, et al. Geochronological study on Yazigou polymetallic deposit in Eastern Kunlun, Qinghai Province[J]. *Acta Geologica Sinica*, 2008, 82(7): 949–955(in Chinese with English abstract).
- [30] 南卡俄吾, 贾群子, 李文渊, 等. 青海东昆仑哈西亚图铁多金属矿区石英闪长岩LA–ICP–MS锆石U–Pb年龄和岩石地球化学特征[J]. *地质通报*, 2014, (6): 841–849.
- Namka Norbu, Jia Qunzhi, Li Wenyuan, et al. LA–ICP–MS zircon U–Pb age and geochemical characteristics of quartz diorite from the Haxiyatu iron– polymetallic ore district in Eastern Kunlun [J]. *Geological Bulletin of China*, 2014, (6): 841–849 (in Chinese with English abstract).
- [31] 孔会磊, 李金超, 栗亚芝, 等. 青海东昆仑东段按纳格闪长岩地球化学及锆石U–Pb年代学研究[J]. *地质科技情报*, 2014, 33(6): 11–17.
- Kong Huilei, Li Jinchao, Li Yanzhi, et al. Geochemistry and zircon U–Pb geochronology of annage diorite in the Eastern Section from East Kunlun in Qinghai Province[J]. *Geological Science and Technology Information*, 2014, 33(6): 11–17 (in Chinese with English abstract).
- [32] 何书跃, 李东生, 李良林, 等. 青海东昆仑鸭子沟斑岩型铜(钼)矿区辉钼矿铼–钨同位素年龄及地质意义[J]. *大地构造与成矿学*, 2009, 33(2): 236–242.
- He Shuyue, Li Dongsheng, Li Lianglin, et al. Re–Os age of molybdenite from the Yazigou copper(molybdenum) mineralized area in Eastern Kunlun of Qinghai Province, and its geological significance[J]. *Geotectonica et Metallogenia*, 2009, 33(2): 236–242(in Chinese with English abstract).
- [33] 宋忠宝, 张雨莲, 陈向阳, 等. 东昆仑哈日扎含矿花岗闪长斑岩LA–ICP–MS锆石U–Pb定年及地质意义[J]. *矿床地质*, 2013, 32(1): 157–168.
- Song Zhongbao, Zhang Yulian, Chen Xiangyang, et al. Geochemical characteristics of Harizha granite diorite–porphyry in East Kunlun and their geological implications[J]. *Mineral Deposits*, 2013, 32(1): 157–168(in Chinese with English abstract).
- [34] 许庆林. 青海东昆仑造山带斑岩型矿床成矿作用研究[D]. 长春: 吉林大学, 2014.
- Xu Qinglin. Study on Metallogenesis of Porphyry Deposits in Eastern Kunlun Orogenic Belt, Qinghai Province[D]. Changchun: Jilin University, 2014(in Chinese with English abstract).
- [35] 殷鸿福, 张克信. 中央造山带的演化及其特点[J]. *地球科学*, 1998, 23(5): 437–442.
- Yin Hongfu, Zhang Kexin. The evolution of the central orogenic belt and its characteristics [J]. *Journal of Earth Science*, 1998, 23(5): 437–442(in Chinese with English abstract).
- [36] Song Shuguang, Niu Yaoling, Su Li, et al. Continental orogenesis from ocean subduction, continent collision/subduction, to orogen collapse, and orogen recycling: The example of the North Qaidam UHPM belt, NW China[J]. *Earth–Science Reviews*, 2014, 129(1): 59–84.
- [37] 许志琴, 姜枚, 杨经绥. 青藏高原北部隆升的深部构造物理作用: 以“格尔木—唐古拉山”地质及地球物理综合剖面为例[J]. *地质学报*, 1996, 70(3): 195–206.
- Xu Zhiqin, Jiang Mei, Yang Jingsui. Tectonophysical process at depth for the uplift of the Northern part of the Qinghai–Tibet Plateau: illustrated by the geological and geophysical comprehensive profile from Golmud to the Tanggula Mountains, Qinghai Province China[J]. *Acta Geologica Sinica*, 1996, 70(3): 195–206 (in Chinese with English abstract).
- [38] Yuan Honglin, Gao Shan, Dai Mengning, et al. Simultaneous determinations of U–Pb age, Hf isotopes and trace element compositions of zircon by excimer laser–ablation quadrupole and multiple–collector ICP–MS[J]. *Chemical Geology*, 2008, 247(1/2):100–118.
- [39] Ludwig K R. Mathematical–statistical treatment of data and errors for $^{230}\text{Th}/\text{U}$ geochronology[J]. *Reviews in Mineralogy & Geochemistry*, 2003, 52(1)631–656.
- [40] Rickwood Peter C. Boundary lines within petrologic diagrams which use oxides of major and minor elements[J]. *Lithos*, 1989, 22(4):247–263.
- [41] Peccerillo Angelo, Taylor S R. Geochemistry of Eocene calc–alkaline volcanic rocks from the Kastamonu area, northern

- Turkey[J]. *Contributions to Mineralogy and Petrology*, 1976,58(1): 63–81.
- [42] Boynton W V. Cosmochemistry of the rare earth elements: meteoric studies[J]. *Rare Earth Element Geochemistry*, 1984:63–114.
- [43] Sun S S, McDonough W F. Chemical and isotopic systematics of oceanic basalts: Implications for mantle composition and processes[J]. *Geological Society of London Special Publications*, 1989,42(1):313–345.
- [44] 吴元保, 郑永飞. 锆石成因矿物学研究及其对U–Pb年龄解释的制约[J]. *科学通报*, 2004,49(16):1589–1604.
Wu Yuanbao, Zheng Yongfei. Zircon genetic mineralogy research and interpretation of U – Pb age restriction[J]. *Chinese Science Bulletin*, 2004,49(16):1589–1604 (in Chinese).
- [45] Yang Shuiyuan, Jiang Shaoyong, Jiang Yaohui, et al. Geochemical, zircon U–Pb dating and Sr–Nd–Hf isotopic constraints on the age and petrogenesis of an Early Cretaceous volcanic–intrusive complex at Xiangshan, Southeast China[J]. *Mineralogy and Petrology*, 2012, 58(11):21–48.
- [46] Claesson S, Vetrin V, Bayanova T, et al. U–Pb zircon ages from a Devonian carbonatite dyke, Kola Peninsula, Russia: A record of geological evolution from the Archaean to The Palaeozoic[J]. *Lithos*, 2000, 51(1): 95–108.
- [47] 李文良, 夏锐, 卿敏, 等. 应用辉钼矿Re–Os定年技术研究青海什多龙砂卡岩型钼铅锌矿床的地球动力学背景[J]. *岩矿测试*, 2014, 33(06): 900–907.
Li Wenliang, Xia Rui, Qing Min, et al. Re–Os molybdenite ages of the shenduolong skarn Mo–Pb–Zn deposit and geodynamic framework, Qinghai Province[J]. *Rock and Mineral Analysis*, 2014, 33(06): 900–907(in Chinese with English abstract).
- [48] Xia Rui, Wang Changming, Qing Min, et al. Molybdenite Re–Os, zircon U–Pb dating and Hf isotopic analysis of the Shuangqing Fe–Pb–Zn–Cu skarn deposit, East Kunlun Mountains, Qinghai Province, China[J]. *Ore Geology Reviews*, 2015, 66: 114–131.
- [49] 孙延贵, 张国伟, 郑健康, 等. 柴达木地块东南缘岩浆弧(带)形成的动力学背景[J]. *华南地质与矿产*, 2001,(04):16–21.
Sun Yangui, Zhang Guowei, Zheng Jiankang, et al. Analysis of dynamic backgrounds of magmatic arc in the southeastern margin of Qaidam massif [J]. *Geology and Mineral Resources of South China*, 2001,(04):16–21(in Chinese with English abstract).
- [50] Frost B Ronald, Barnes Calvin G, Collins William J, et al. A geochemical classification for granitic rocks[J]. *Journal of Petrology*, 2001,42(11):2033–2048.
- [51] Pitcher Wallace Spencer. Granites and yet more granites forty years on[J]. *Geologische Rundschau*, 1987, 76(76):51–79.
- [52] Pearce Julian A, Harris Nigel B W, Tindle Andrew G. Trace element discrimination diagrams for the tectonic interpretation of granitic rocks[J]. *Journal of Petrology*, 1984,25(4):956–983.
- [53] Petford Nick, Atherton Michael. Na–rich partial melts from newly underplated basaltic crust: the Cordillera Blanca Batholith, Peru[J]. *Journal of Petrology*, 1996,37(6):1491–1521.
- [54] Defant Marc J, Mmond Mark S. Derivation of some modern arc magmas by melting of young subducted lithosphere[J]. *Nature*, 1990, 347(6294):662–665.
- [55] 朱弟成, 潘桂棠, 莫宣学, 等. 冈底斯中北部晚侏罗世—早白垩世地球动力学环境:火山岩约束[J]. *岩石学报*, 2006, 22(3): 534–546.
Zhu Dicheng, Pan Guitang, Mo Xuanxue, et al. Late Jurassic–Early Cretaceous geodynamic setting in middle– northern Gangdese: New insights from volcanic rocks[J]. *Acta Petrologica Sinica*, 2006, 22(3): 534–546(in Chinese with English abstract).
- [56] Rapp Robert P, Watson E. Bruce. Dehydration Melting of Metabasalt at 8–32 kbar: Implications for continental growth and crust–mantle recycling[J]. *Journal of Petrology*, 1995, 36(4): 891–931.
- [57] Barth Matthias G, Nough William F, Rudnick Roberta L. Tracking the budget of Nb and Ta in the continental crust[J]. *Chemical Geology*, 2000, 165(99):197–213.
- [58] Sun S S, McDonough W F. Chemical and isotopic systematics of oceanic basalts: Implications for mantle composition and processes[J]. *Geological Society of London Special Publications*, 1989,42:313–345.
- [59] Sisson T W, Ratajeski K, Hankins W B, et al. Voluminous granitic magmas from common basaltic sources[J]. *Contributions to Mineralogy & Petrology*, 2005, 148(6): 635–661.
- [60] Douce Alberto E, Patiño, Johnston A. Dana. Phase equilibria and melt productivity in the pelitic system: implications for the origin of peraluminous granitoids and aluminous granulites[J]. *Contributions to Mineralogy & Petrology*, 1991, 107(2): 202–218.
- [61] Roberts Malcolm P, Clemens John D. Origin of high–potassium, calc–alkaline, I–type granitoids[J]. *Geology*, 1993, 21(9): 825.
- [62] 莫宣学, 罗照华, 邓晋福, 等. 东昆仑造山带花岗岩及地壳生长[J]. *高校地质学报*, 2007, 13(3): 403–414.
Mo Xuanxue, Luo Zhaohua, Deng Jinfu, et al. Granite and crustal growth orogenic belt of East Kunlun[J]. *Geological Journal of China Universities*, 2007, 13(3): 403–414(in Chinese with English abstract).
- [63] 熊富浩. 东昆仑造山带东段古特提斯域花岗岩类时空分布、岩石成因及其地质意义[D]. 中国地质大学(武汉), 2014.
Xiong Fuhao. Spatial– temporal Pattern, Petrogenesis and Geological Implications of Pale–Tethyan Granitoids in the East Kunlun Orogenic Belt (Eastern Segment) [D]. *China University of Geosciences(Wuhan)*, 2014(in Chinese with English abstract).
- [64] 郭正府, 邓晋福, 许志琴, 等. 青藏东昆仑晚古生代末—中生代中酸性火成岩与陆内造山过程[J]. *现代地质*, 1998, 12(3):344–352.
Guo Zhengfu, Deng Jinfu, Xu Zhiqin, et al. Late Palaeozoic–mesozoic intracontinental orogenic process and iniermediate – acidic igneous rocks from the Eastern Kunlun Mountains of Northwestern China[J]. *Geoscience*, 1998,12(3): 344– 352(in Chinese with English abstract).
- [65] 孙延贵. 西秦岭—东昆仑造山带的衔接转换与共和坳拉谷[D]. 西安:西北大学, 2004.
Sun Yangui. Gonghe Aulacogen and Conjugate and Transfer between the West Qinling and East Kunlun orogens [D]. Xi’an: Northwest University, 2004(in Chinese with English abstract).